Cite this: DOI: 10.1039/c0xx00000x

www.rsc.org/xxxxxx

ARTICLE TYPE

Direct preparation and conversion of copper hydroxide-based monolithic xerogels with hierarchical pores

Shotaro Fukumoto,[a] Kazuki Nakanishi*[a] and Kazuyoshi Kanamori[a]

Received (in XXX, XXX) Xth XXXXXXXXX 20XX, Accepted Xth XXXXXXXXX 20XX

DOI: 10.1039/b000000x

Copper hydroxide-based monolithic xerogels with controlled hierarchical pores have been prepared directly by a sol-gel process from an ionic precursor, $CuCl_2 \cdot 2H_2O$. Propylene oxide acts as a gelation inducer by increasing pH homogeneously in a reaction solution. Poly(acrylamide) is utilized not only to control macroscopic phase separation but also to support the network physically. Glycerol contributes to formation of monolithic gels by suppressing the crystal growth of copper hydroxide. Appropriate starting composition leads to co-continuous gel skeletons and macropores. Though the as-dried gels were amorphous, post-treatments (calcination and solvothermal treatment) formed metallic copper and copper oxides (CuO and Cu_2O) without collapse of monolithic form and macrostructure.

Introduction

Porous materials are expected in various applications such as catalysis, adsorption, separation, electrodes, and insulation, and are playing a crucial role in the development of materials for the sustainable society.[1-4] Although several material forms such as particles and films are widely studied, monolithic porous materials attract increasing attention due to their easy handling and potential for, for example, separation media[5,6] and efficient column-type contact devices such as monolithic flow-through reactors.[7,8] Recently, there have been many preparation methods of monolithic porous materials such as nanocasting,[9] foaming,[10,11] replication/sacrificial templating,[11] and sol-gel processing accompanied by phase separation.[5,12] The typical nanocasting method uses a hard silica template and the silica has to be removed by a severe condition using such as strong base and hydrofluoric acid.[9] A sol-gel process accompanied by phase separation, which has been developed in alkoxysilane-derived sol-gel systems, enables a spontaneous formation of macroporous monoliths and there is no need to use those harmful reagents as well as template. In this method, controlled phase separation is induced in the course of hydrolysis and polycondensation of precursor, and well-defined co-continuous macroporous structure can be obtained by freezing the temporal coarsening structure of spinodal decomposition by the sol-gel transition.[12] The macroporous morphology can be tuned predominantly with concentration of phase-separation inducer, e.g. water-soluble polymers and surfactants. Mesopores, which enhance surface area, can be added in the macropore skeletons by a dissolution-reprecipitation-based post treatment[13] (Ostwald ripening) and/or soft templating using a structure-directing agent.[14] In addition, micropores can also be tailored by selecting microporous frameworks such as activated carbons, zeolites.[15-17]

For more rational design of porous materials with desired chemical composition, besides, diversity of derivatives would be another key point. In other words, the parent material should be transformed into different compounds/composites by a post treatment such as solvothermal treatment and calcination in a controlled atmosphere. We have reported metal (oxy)hydroxide-based porous monoliths (the metal species include titanium,[18,19] aluminum,[20] zirconium,[21] iron,[22] nickel,[23] and chromium[24]) that can be converted into oxygen-deficient metal oxides,[25,26] elemental metals, metal carbides, metal nitrides, and their composites with carbons. Many of these metal oxide-related materials have been achieved by an extension of the epoxide-mediated sol-gel process from ionic precursors,[27-29] rather than highly reactive metal alkoxide-derived systems. The epoxide-mediated sol-gel process utilizes an irreversible opening reaction of epoxide, which consumes proton in a solution to swiftly and uniformly raise the solution pH. Hydrolysis and condensation of aquo metal cations occur simultaneously and metal (oxy)hydroxide networks are formed as a result.[27-29] Further development of this strategy would allow us to prepare macroporous monoliths of various trivalent metal oxides, divalent oxides and mixed metal oxides. In comparison to the previous works, however, it is increasingly difficult to prepare copper-based monolithic gels, because coordination polyhedra of divalent cations are less stable than trivalent ones,[30] and it is hard to control the rate of precipitation-sedimentation against that of monolithic gel network formation.

Copper-based materials have been utilized in various applications such as catalysts[31-33] and semiconductors.[34] The controls over valence state and composition of the copper-based materials are particularly important in practical applications including abovementioned ones. Porous copper oxide materials reported in the previous work[35] are presumed to be aggregates of precipitates rather than homogeneously crosslinked monoliths (after being used as a catalyst, centrifugation was required to

separate the material probably due to its very low mechanical strength.), and their macropores are uncontrolled. In this work, we report a direct preparation of porous copper hydroxide-based monolithic xerogels with controlled macro/mesopores and their conversions to copper-based materials with various valence states from Cu(0) to Cu(II). The copper hydroxide-based porous monolithic materials have been successfully prepared with the aid of organic additives that prevent undesirable crystallization and reinforce the network.[22-24] The effects of change in the starting composition and the role of one of the additives (glycerol) on the gel morphology and the crystal growth have been investigated in detail. Heat treatment in oxidative and inert atmospheres at different temperatures has been found to yield the different crystalline phases, e.g. metallic copper and copper oxides (CuO and Cu_2O). In addition, solvothermal treatment in ethylene glycol has also reduced to metallic copper under a milder condition. Pore properties and monolithicity are also influenced by these post-treatment processes.

Table 1 Starting compositions of samples.

Sample ID	$CuCl_2$•$2H_2O$ /g	Water[a] /mL (Total)	Ethanol /mL	GLY /mL	PAAm[b] /g (Absolute)	PO /mL
C1	1.53	1.1	0.3	2.4	0.5	1.47
C2	1.53	1.1	0.3	2.4	0.6	1.47
C3	1.53	1.1	0.3	2.4	0.7	1.47
C4	1.53	1.1	0.3	2.4	0.8	1.47
C5	1.53	1.1	0.3	2.4	0.9	1.47
C6	1.53	1.2	0.3	2.4	0.6	1.47
C7	1.53	1.2	0.3	2.4	0	1.47
C8	1.53	3.6	0.3	0	0.6	1.47
C9	1.53	3.6	0.3	0	0	1.47

PAAm is in 50 wt% in water, so [a] the total volume of water is $V_{water} + W_{PAAm} \times 1/2$, assuming water density ~ 1 g cm^{-3} and [b] the absolute weight of PAAm is $W_{PAAm} \times 1/2$.

Experimental

Synthesis

Copper(II) chloride dihydrate ($CuCl_2$•$2H_2O$: Sigma-Aldrich Co., USA, 98 %) was used as a copper source. Distilled water, ethanol (Kishida Chemical, Japan, ≥99.5 %), and glycerol (GLY: Kishida Chemical, Japan, ≥99.0 %) were used as the solvent mixture. Poly(acrylamide) (PAAm: Sigma-Aldrich Co., USA, 50 wt % in water) with average molecular weight of 10,000 was used to control macroscopic phase separation. Propylene oxide (PO: Sigma-Aldrich Co., USA, ≥99 %) was added to promote gelation by enhancing hydrolysis of copper aquo ions. To wash the as-prepared samples, 2-Propanol (IPA: Kishida Chemical, Japan, ≥99.0 %) was used. Ethylene glycol (EG: Kishida Chemical, Japan, ≥99.5 %) was used for solvothermal treatment.

Sample gels were prepared with the starting compositions listed in Table 1. First, 1.53 g of $CuCl_2$•$2H_2O$ and W_{PAAm} g of aqueous PAAm solution were dissolved in a mixture of V_{water} mL of distilled water, $V_{ethanol}$ mL of ethanol and V_{GLY} mL of glycerol. Then, 1.47 mL of PO was added under stirring at an ambient temperature (25 °C). After stirring for 1 min, the homogeneous solution thus prepared was sealed and kept at 30 °C for gelation. The wet gels, typically obtained after 10–15 min, were aged at 30 °C for 24 h and immersed in IPA at 60 °C for 24 h three times and then dried by evaporation at 60 °C.

Some samples were calcined at different temperatures for 4 h with a heating rate of 4 °C min^{-1} in air or argon stream at a rate of 1 L min^{-1} in an electric furnace. Some samples calcined in argon were further calcined at 400 °C for 4 h with a heating rate of 4 °C min^{-1} in air to remove the remnant carbons.

Some wet gel samples immersed in ethylene glycol after gelation were subjected to the solvothermal treatment in an autoclave heated at 180 °C for various durations up to 6 h.

Characterizations.

Morphology of the dried gels and heat-treated gels was observed by a scanning electron microscope (SEM: JSM-6060, JEOL, Ltd., Japan, with Pt coating). Thermogravimetry-differential thermal analysis (TG-DTA: Thermo plus TG 8120, Rigaku Corp., Japan) up to 600 °C was performed at a heating rate of 5 °C min^{-1} while continuously supplying air at the rate of 100 mL min^{-1}. Molecular-level information on the sample was investigated with Fourier transform infrared spectroscopy (FT-IR: IR Affinity-1, Shimadzu Corp., Japan) using the conventional pellet technique with potassium bromide (KBr); the spectra were collected with 100 scans for the wavenumber range 400−4000 cm^{-1} at a resolution of 2 cm^{-1}. The X-ray diffraction (XRD) analysis was carried out with a RINT system (2θ from 10 ° to 90 °, 1.6 kW, CuKα: λ = 0.154 nm, RINT-Ultima III, Rigaku Corp., Japan). Micro/mesopores were characterized by the nitrogen adsorption−desorption technique (BELSORP-mini II, Bel Japan Inc., Japan). Before measurement, each sample was degassed at 80 °C under vacuum for more than 4 h. Surface area was obtained by the Brunauer−Emmett−Teller (BET) method.

Results and discussion

Effect of PAAm on the Gel Morphology.

The starting solutions with the compositions listed in Table 1 were homogeneous and transparent green in color. The addition of PO quickly resulted in the formation of copper hydroxide-based gels (~13 min in C3),[36,37] while no gelation was observed without an addition of PO.

Figure 1(a) shows appearance of a dried gel, and Figure 1(b)-(f) shows SEM images of the dried gels prepared with varied W_{PAAm}. The total volume of water, ($V_{water} + W_{PAAm} \times 1/2$, assuming water density ~ 1 g cm^{-3}), was set at 1.1 mL for C1 to

C5.

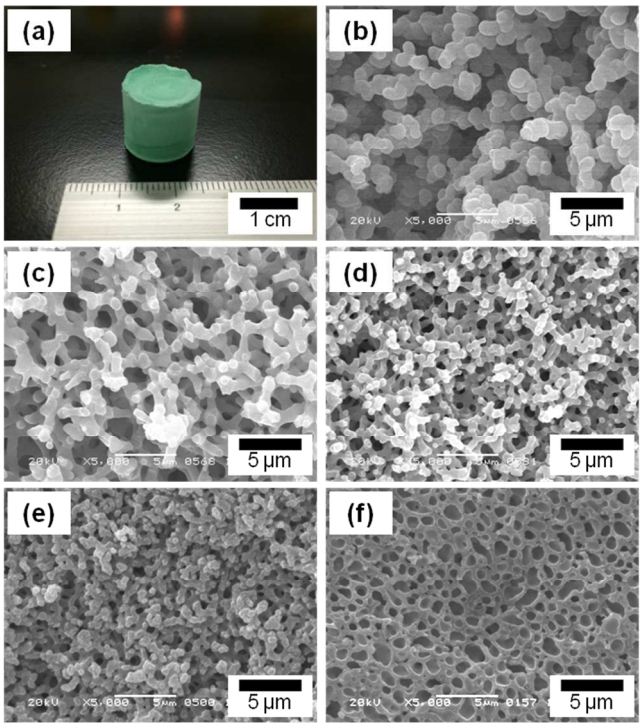

Fig. 1 Appearance of a resultant dried gel (a), SEM images of the samples prepared with varied starting compositions: (b) C1, (c) C2, (d) C3, (e) C4, and (f) C5. Detailed starting compositions are listed in Table 1.

In the absence of PAAm, no gelation was observed but dispersed precipitates were formed. On the other hand, with PAAm, monolithic gels were formed and their morphologies varied depending on W_{PAAm}. In C1, the gel skeleton exhibits a co-continuous structure consisting of similar-sized globular units (Figure 1(b)), whereas the appropriate amount of W_{PAAm} leads to co-continuous gel skeletons with smoother surface (C2, Figure 1(c)). A further increase of W_{PAAm} makes macropore size smaller (C3, Figure 1(d) and C4, Figure 1(e)), which means PAAm suppresses the progress of phase separation. The addition of an excessive amount of PAAm resulted in the morphology with isolated macropores (C5, Figure 1(f)). Moreover, with an increasing amount of PAAm, the volume fraction of macropore skeletons are increased, which indicates that PAAm is preferentially incorporated in the skeletons.

For the purpose of clarifying the role of PAAm, we carried out thermal analysis and molecular-level structural analysis, through which the distribution of PAAm between gel phase and solvent phase has been determined. The TG-DTA curves of the gels prepared with a smaller amount of PAAm (C1) and larger amount (C5) are depicted in Figure 2(a). The curves show that the weight loss of the gel has a reasonable correlation with the amount of PAAm contained in the starting compositions. Exothermic peaks around 200 °C and 350 °C are ascribed to the combustion of glycerol and PAAm, respectively.[22,38] The FT-IR spectrum of C6 is shown in Figure 2(b). The presence of PAAm in the gel skeletons is confirmed by the peaks derived from the primary amide group of PAAm: deformation vibration of –NH groups (1,200 cm^{-1}), stretching vibration of C-N bonds (1,450 cm^{-1}), bending vibration of N-H bonds (1,604 cm^{-1}), stretching vibration of C=O groups (1,658 cm^{-1}), and stretching vibration of N-H bonds (3,186 cm^{-1}).[39-42]

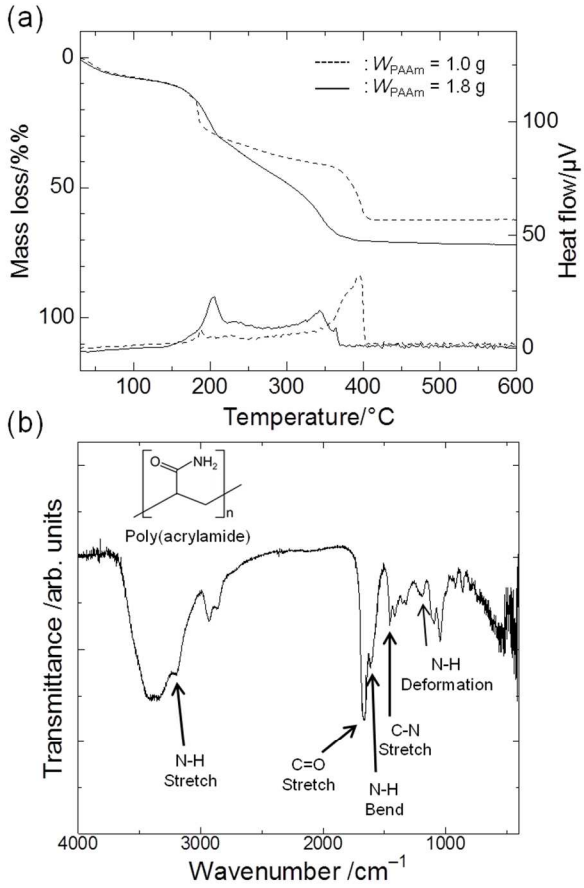

Fig. 2 (a) TG-DTA curves of the gel-phase of dried samples prepared with a smaller amount of PAAm (C2, dashed lines) and a larger amount (C4, solid lines). (b) FT-IR spectrum of C6.

The homogeneous solution separates into two phases one rich in PAAm-copper(II) hydroxide-based composite (gel-phase) and the other rich in the solvent mixture (solvent-phase), and the sol-gel transition arrests the transient phase-separating structure.[12] Both PAAm and copper(II) hydroxide can interact each other strongly by hydrogen bonds between amide groups and hydroxyl groups or by coordinate bonds between nitrogen in amide groups and copper ions.[43] After removal of solvent by evaporative drying, the spaces occupied by the solvent-phase become macropores. It was previously reported that in iron(III) hydroxide systems, PAAm acts not only in controlling phase separation but also in physically supporting the network.[22] Also in the present case, PAAm plays double role similarly to the case of iron(III) hydroxide system.

Effect of Glycerol on the Crystallization.

Figure 3(a) shows XRD patterns of the samples prepared with glycerol and PAAm (C6, i), with glycerol and without PAAm (C7, ii), without glycerol and with PAAm (C8, iii), and without glycerol and PAAm (C9, iv). C6 is monolithic gel with co-continuous macropore (Figure 5.c(i)). The total volume of solvent, (V_{water} + W_{PAAm} × 1/2 + V_{GLY}), was set at 3.6 mL for C6

to C9.

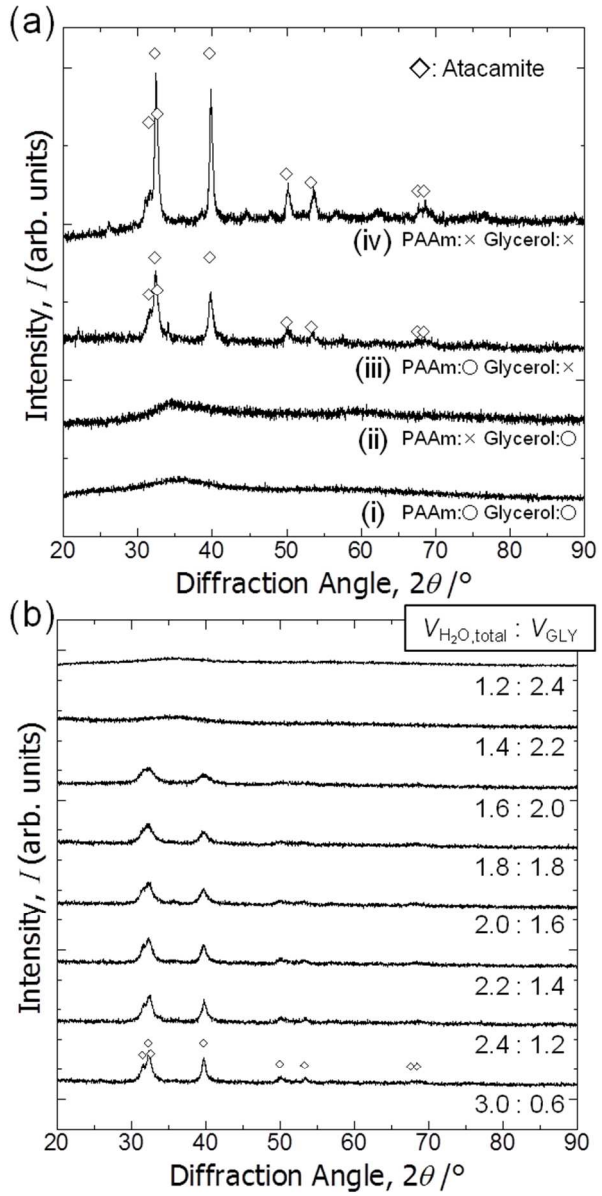

Fig. 3 (a) X-ray diffraction patterns of the samples prepared with or without glycerol and PAAm: (i) C3, (ii) C1, (iii) C9, and (iv) C10. (b) X-ray diffraction patterns of the samples prepared with varied V_{H2O}:V_{GLY} ratio.

Regardless of the presence of PAAm, no obvious diffraction peaks are found in the samples prepared with glycerol. It should be pointed out that the crystalline phase is atacamite ($Cu_2(OH)_3Cl$) [PDF#00-023-0948], suggesting a considerable amount of Cl^- is incorporated in the original gel structure. This means that some chloride anions coordinate copper cations and do not react with PO. Figure 3(b) shows XRD patterns of the samples prepared with varied V_{water} and V_{GLY}, setting the total volume of solvents, (V_{H2O} + W_{PAAm} × 1/2 + V_{GLY}), constant at 3.6 mL. With an increase of V_{GLY}, the diffraction peaks changes into those with lower intensity and larger width, and no obvious peaks are found in the samples prepared with more than 2.2 mL of glycerol, which indicates glycerol prevents the crystal growth. Samples prepared with less than 2.0 mL of glycerol are precipitates but do not form monolith, whereas with more than 2.2 mL of glycerol the monolithic wet gels have been obtained. In addition, atacamite is known to form plate-like crystals, which means that the suppression of crystal growth by glycerol allows the network to expand in three-dimensional and monolithic gels are formed. Zhao et al. also reported the suppression of crystal growth of magnetites by polyols, which can be attributed to limited dissolution-reprecipitation and binding of polyols on the crystal surface.[44]

Crystal Phase Transition by Calcination.

The XRD patterns of the samples calcined under varied calcination temperature in air are depicted in Figure 4(a). The calcination was performed on the gel prepared with the starting composition C6. The as-dried gel exhibits no obvious diffractions, indicating that only amorphous and/or nanocrystalline phases undetectable by XRD are contained. After calcination in air at 100 °C, the gel remains amorphous, whereas at 200 °C diffraction peaks from mixed phases appear, and at 300 °C, peaks ascribed to copper(II) oxide becomes evident. After calcination at 200 °C or 300 °C, the monolithic form was not preserved. We assume that the burn-off of PAAm, which had firmly supported the gel skeletons through the strong interactions, has resulted in the collapse of the monolithic form of the gel pieces. Figure 4(b) shows XRD results of the samples calcined at varied temperatures in argon. Again, the calcination was performed on C6 gels. At 200 °C, the metallic copper phase is recognized.[45] As the calcination temperature is increased, the peaks becomes sharper and stronger until 800 °C. At 1000 °C, near the melting point of copper, the peak growth is no longer seen probably due to the partial melting of grown copper crystals. Although calcination in argon causes overall shrinkage, complete burn-off of PAAm is prevented and instead carbonized materials are left within the skeleton. Because of uniformly distributed carbon in the skeletons, the monolithic form and microstructure have been preserved (Figure 4(c (ii))).[22-24] The carbons derived from the organic species not only act as a network supporter but also as a reducing agent, leading to the metallic copper phase.[45] The absence of bulk electrical conductivity of metallic copper – carbon composite thus prepared indicates that the copper phase exists in a non-percolating manner. In order to confirm the morphological and compositional changes, we calcined samples firstly in argon at 800 °C, followed by in air at 400 °C to burn off the carbons. The gel skeletons are considered to be densified after the shrinkage during calcination in argon accompanied by the collapse of mesopores (Figure 5). As a result, the monolithic form has been preserved (Figure 4(c (iii))) in the sample, which consists of copper(II) oxide (Figure S1, ESI†). In this case, almost all of carbon was burn off (Figure S2, ESI†). Through the successive heat-treatment, macroporous monoliths of copper/carbon composite and copper(II) oxide can be selectively prepared.

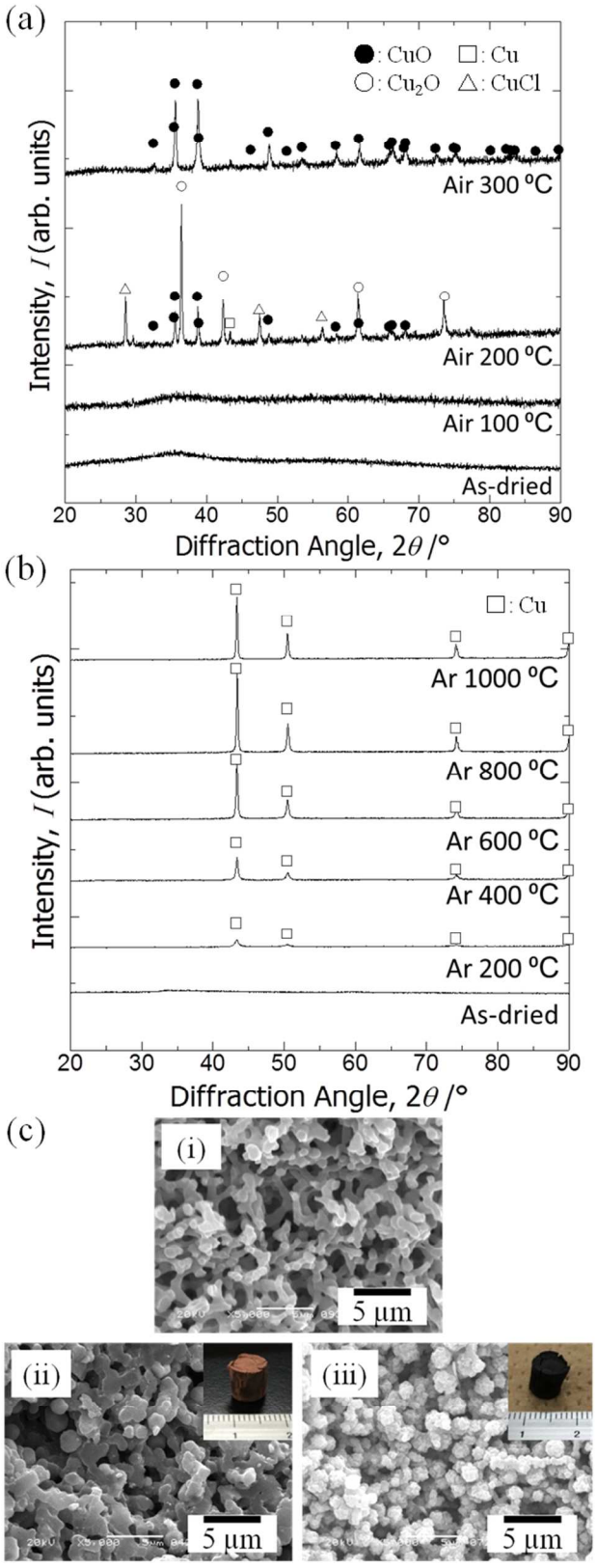

Fig. 4 X-ray diffraction patterns of the samples: (a) as-dried one and those calcined in air at different temperatures, (b) as-dried and calcined in argon at different temperatures. Symbols indicate open square: Cu [PDF#00-004-0836], open triangle: CuCl [PDF#01-081-1841], closed circle: CuO [PDF#00-048-1548], and open circle: Cu_2O [PDF#01-073-6371] respectively. (c) SEM images of the samples; (i) as-dried, (ii) calcined in argon at 800 °C and (iii) calcined in argon at 800 °C and successively in air at 400 °C. Insets show the appearance of each sample.

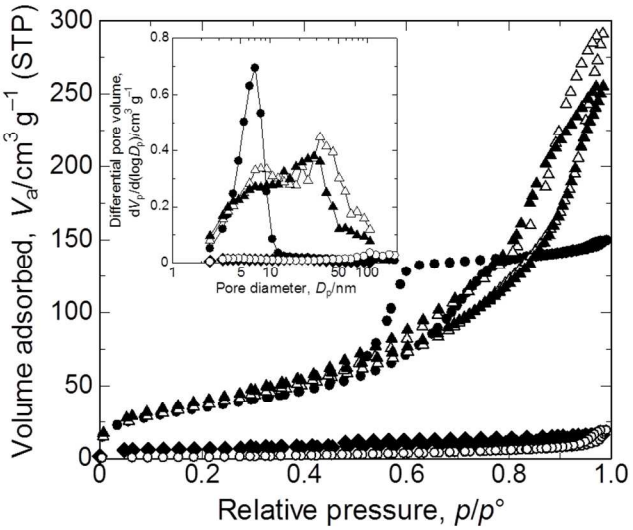

Fig. 5 Nitrogen adsorption-desorption isotherms of the as-dried and heat-treated samples. Symbols indicate closed circle: as-dried, closed rhombus: calcined in argon at 800 °C, open circle: calcined in argon at 800 °C followed by in air at 400 °C, open triangle: solvothermally-treated for 2 h, and closed triangle: solvothermally-treated for 6 h. Inset shows the BJH pore distributions. Refer to Table 2 for details in pore parameters.

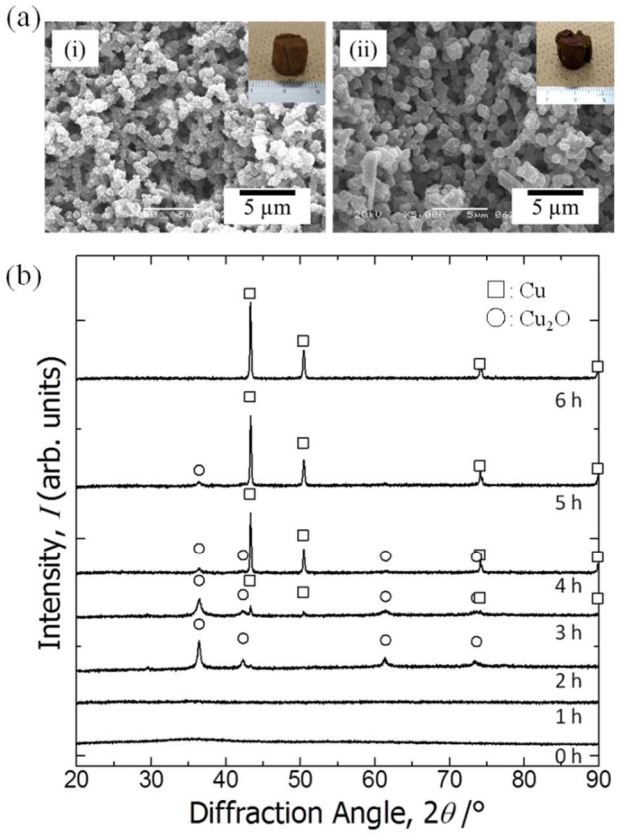

Fig. 6 (a) SEM images of the samples treated in a solvothermal condition in ethylene glycol for various durations: (i) 2 h (EG2 in Table 2), and (ii) 6 h (EG6). Insets of (i) and (ii) show their appearance. (b) X-ray diffraction patterns of the samples: as-dried and solvothermally-treated in

ethylene glycol for various durations. Symbols indicate open square: Cu, and open circle: Cu_2O.

Solvothermal Treatment

Since samples calcined in argon at 200 °C contain the copper(0) phase, we assumed that copper ions in the as-dried samples are in the state easy to be reduced. We then tried solvothermal treatment, which is a milder reducing process,[46-48] in ethylene glycol as the reducing agent to obtain macroporous metallic Cu and Cu_2O monoliths.[49,50] As a result, we not only could preserve the monolithic form and microstructure (Figure 6(a)), but also obtain a reduced states of copper depending on the duration of the treatment (Figure 6(b)). Unlike calcination, since apparent shrinkage does not occur, mesopores of the samples are well preserved (Figure 5). It is therefore an superior process to obtain hierarchically macro- and mesoporous copper(I) oxide/PAAm composite and metallic copper/PAAm composite gels.

Table 2 Summary of the obtained samples. (Symbols correspond to those in Figure 5)

Symbol	Sample ID	mesopore size / nm	S_{BET} / m^2 g^{-1}	pore volume/ cm^3 g^{-1}	constituent elements	microstructure
●	C6	7	127	0.24	amorphous atacamite / PAAm	macro-mesoporous
◆	Ar800	-	21	0.02	copper(0) / carbon	macroporous
○	Ar800+Air400	-	5	0.03	copper(II) oxide	macroporous
△	EG2	33	138	0.46	copper(I) oxide / PAAm	macro-mesoporous
▲	EG6	28	149	0.40	copper(0) / PAAm	macro-mesoporous

.

Conclusions

Copper-based xerogel monoliths with macropores have been prepared using copper salt as a precursor in an epoxide-mediated sol-gel process accompanied by phase separation. Glycerol in the starting solution is incorporated in the gel skeletons and suppresses crystallization-precipitation of the copper hydroxide-based network, and poly(acrylamide) (PAAm) is also incorporated in the gel skeletons and acts not only in controlling phase separation but also in physically supporting the network. Appropriate starting compositions allow the concurrent phase separation and gelation, leading to the formation of macroporous gels with co-continuous structure. By calcination in air, copper(II) oxide phase appears, while the monolithic form has been collapsed. By calcination in argon, copper(0)/carbon macroporous monoliths have been obtained. The as-dried gels are reduced and metallic copper phase appears with keeping the microstructure and monolithic form, while mesopores are collapsed due to shrinkage. Successive calcination in air of the samples calcined in argon results in crystallization into copper(II) oxide with keeping the macroporous morphology and monolithic form (CuO macroporous monoliths). By solvothermal treatment in ethylene glycol, copper(0)/PAAm and copper(I) oxide/PAAm macro/mesoporous monoliths have been obtained with preserving most of the mesopores and monolithic form. Another important transformation of the as-dried gels into porous coordination polymers/metal organic frameworks (PCPs/MOFs) is reported elsewhere in parallel with the present paper.[51] The present comprehensive strategy to the monolithic porous materials with different copper-based phases ensures different applications such as in catalysis, electrochemical devices and separations.

Notes and references

[a] *Department of Chemistry, Graduate School of Science, Kyoto University, Kitashirakawa, Sakyo-ku, Kyoto 606-8502, Japan. Fax/Tel: +81 757 532 925; E-mail: kazuki@kuchem.kyoto-u.ac.jp*

† Electronic Supplementary Information (ESI) available: X-ray diffraction patterns of the samples calcined in argon at 800 °C followed by in air at 400 °C, and TG-DTA curves of the sample calcined in argon at 800 °C and one calcined in argon at 800 °C followed by in air at 400 °C. See DOI: 10.1039/b000000x/

1 R. J. White, R. Luque, V. L. Budarin, J. H. Clark and D. J. Macquarrie, *Chem. Soc. Rev.,* 2009, **38**, 481.
2 J. R. Li, R. J. Kuppler and H. C. Zhou, *Chem. Soc. Rev.* 2009, **38**, 1477.
3 C. Sanchez, P. Belleville, M. Popall and L. Nicole, *Chem. Soc. Rev.* 2011, **40**, 696.
4 S. L. Candelaria, Y. Shao, W. Zhou, X. Li, J. Xiao, J. G. Zhang, Y. Wang, J. Liu, J. Li and G. Cao, *Nano Energy* 2012, **1**, 195.
5 K. Nakanishi and N. Tanaka, *Acc. Chem. Res.* 2007, **40**, 863.
6 F. Svec, *J. Chromatogr. A* 2010, **1217**, 902.
7 G. Jas and A. Kirschning, *Chem. Eur. J.* 2003, **9**, 5708.
8 A. Sachse, A. Galarneau, F. Fajula, F. Di Renzo, P. Creux, B. Coq, *Microporous Mesoporous Mater.* 2011, **140**, 58.
9 A. Lu and F. Schüth, *Adv. Mater.* 2006, **18**, 1793.
10 N. Brun, S. Ungureanu, H. Deleuze and R. Backov, *Chem. Soc. Rev.* 2011, **40**, 771.
11 A. R. Studart, U. T. Gonzenbach, E. Tervoort and L. J. Gauckler, *J. Am. Ceram. Soc.* 2006, **89**, 1771.
12 K. Nakanisi, *J. Porous. Mater.* 1997, **4**, 67.
13 K. Nakanishi, R. Takahashi, T. Nagakane, K. Kitayama, N. Koheiya, H. Shikata and N. Soga, *J. Sol-Gel Sci. Technol.* 2000, **17**, 191.
14 T. Amatani, K. Nakanishi, K. Hirao and T. Kodaira, *Chem. Mater.* 2005, **17**, 2114.
15 Y. Tokudome, K. Nakanishi, S. Kosaka, A. Kariya, H. Kaji and T. Hanada, *Microporous Mesoporous Mater.* 2010, **132**, 538.
16 G. Hasegawa, K. Kanamori, K. Nakanishi and T. Hanada, *Carbon* 2010, **48**, 1757.
17 G. Hasegawa, K. Kanamori, K. Nakanishi and T. Hanada, *Chem. Commun.* 2010, **46**, 8037.
18 J. Konishi, K. Fujita, K. Nakanishi and K. Hirao, *Chem. Mater.* 2006, **18**, 6069.
19 G. Hasegawa, K. Kanamori, K. Nakanishi and T. Hanada, *J. Am. Ceram. Soc.* 2010, **93**, 3110.
20 Y. Tokudome, K. Fujita, K. Nakanishi, K. Miura and K. Hirao, *Chem. Mater.* 2007, **19**, 3393.
21 J. Konishi, K. Fujita, S. Oiwa, K. Nakanishi and K. Hirao, *Chem. Mater.* 2008, **20**, 2165.

22 Y. Kido, K. Nakanishi, A. Miyasaka and K. Kanamori, *Chem. Mater.* 2012, **24**, 2071.

23 Y. Kido, K. Nakanishi, N. Okumura and K. Kanamori, *Microporous Mesoporous Mater.* 2013, **176**, 64.

24 Y. Kido, G. Hasegawa, K. Kanamori and K. Nakanishi, *J. Mater. Chem. A* 2014, **2**, 745.

25 A. Kitada, G. Hasegawa, Y. Kobayashi, K. Kanamori, K. Nakanishi and H. Kageyama, *J. Am. Chem. Soc.* 2012, **134**, 10894 .

26 A. Kitada, G. Hasegawa, Y. Kobayashi, K. Miyazaki, T. Abe, K. Kanamori, K. Nakanishi and H. Kageyama, *RSC Adv.* 2013, **3**, 7205.

27 H. Itoh, T. Tabata, M. Kokitsu, N. Okazaki, Y. Imizu and A. Tada, *J. Ceram. Soc. Jpn.* 1993, **101**, 1081-1083.

28 A. E. Gash, T. M. Tillotson, J. H., Jr. Satcher, J. F. Poco, L. W. Hrubesh and R. L. Simpson, *Chem. Mater.* 2001, **13**, 999.

29 A. E. Gash, T. M. Tillotson, J. H., Jr. Satcher, L. W. Hrubesh and R. L. Simpson, *J. Non-Cryst. Solids* 2001, **285**, 22.

30 P. W. Atkins, T. L. Overton, J. P. Rourke, M. T. Weller and F. A. Armstrong, *Inorganic Chemistry,* fifth ed.; Oxford University Press: Oxford, 2010; pp 123

31 K. L. Hohn and Y. C. Lin, *ChemSusChem* 2009, **2**, 927.

32 S. Sá, H. Silva, L. Brandão, J. M. Sousa and A. Mendes, *Appl. Catal. B: Environ.* 2010, **99**, 43.

33 S. Gaillard, C. S. J. Cazin and S. P. Nolan, *Acc. Chem. Res.* 2012, **45**, 778.

34 E. Fortunato, P. Barquinha and R. Martins, *Adv. Mater.* 2012, **24**, 2945.

35 G. A. Naikoo, R. A. Dar and F. Khan, *J. Mater. Chem.* A 2014, **2**, 11792

36 Y. Liu, W. Ren and H. Cui, *Micro Nano Lett.* 2011, **6**, 823.

37 A. Du, B. Zhou, J. Shen, S. Xiao, Z. Zhang, C. Liu and M. Zhang, *J. Non-Cryst. Solids* 2009, **355**, 175.

38 M. Tutas, M. Saglam, M. Yuksel and C. Guler, *Thermochim. Acta* 1987, **111**, 121.

39 S. Rajendran, B. V. Apparao and N. Palaniswamy, *Electrochim. Acta* 1998, **44**, 533.

40 H. Kasgöz, S. Özgümüş and M. Orbay, *Polymer* 2003, **44**, 1785.

41 J. F. Zhu, Y. J. Zhu, M. G. Ma, L. X. Yang and L. Gao, *J. Phys. Chem. C* 2007, **111**, 3920.

42 R. M. Silverstein, F. X. Webster, D. J. Kiemle, Infrared Spectrometry: Spectrometric Identification of Organic Compounds, seventhed.; John Wiley & Sons, Inc.: New York, 2005; pp 99−101.

43 B. L. Rivas, E. D. Pereira and I. Moreno-Villoslada, *Prog. Polym. Sci.* 2003, **28**, 173

44 L. Zhao, H. Zhang, Y. Xing, S. Song, S. Yu, W. Shi, X. Guo, J. Yang, Y. Lei and F. Cao, F. *Chem. Mater.* 2008, **20**, 198.

45 B. V. L'vov, *Thermochim. Acta* 2000, **360**, 109.

46 Y. Zheng, L. Zheng, Y. Zhan, X. Lin, Q. Zheng and K. Wei, *Inorg. Chem.* 2007, **46**, 6980.

47 C. Nethravathi and M. Rajamathi, *Carbon* 2008, **46**, 1994.

48 X. M. Chen and M. L. Tong, *Acc. Chem. Res.* 2007, **40**, 162.

49 S. J. Chen, X. T. Chen, Z. Xue, L. H. Li, and X. Z. You, *J. Cryst. Growth* 2002, **246**, 169.

50 M. Wei, N. Lun, X. Ma and S. Wen, *Mater. Lett.* 2007, **61**, 2147.

51 N. Moitra, S. Fukumoto, J. Reboul, K. Sumida, Y. Zhu, K. Nakanishi, S. Kitagawa, S. Furukawa and K. Kanamori, *Chem. Commun.*, 2015, **51,** 3511

Electronic Supplementary Information

Direct preparation and conversion of copper-based monolithic xerogels with hierarchical pores

Shotaro Fukumoto,[a] Kazuki Nakanishi*[a] and Kazuyoshi Kanamori[a]

[a] Department of Chemistry, Graduate School of Science, Kyoto University,
Kitashirakawa, Sakyo-ku, Kyoto 606-8502, Japan
*E-mail: kazuki@kuchem.kyoto-u.ac.jp

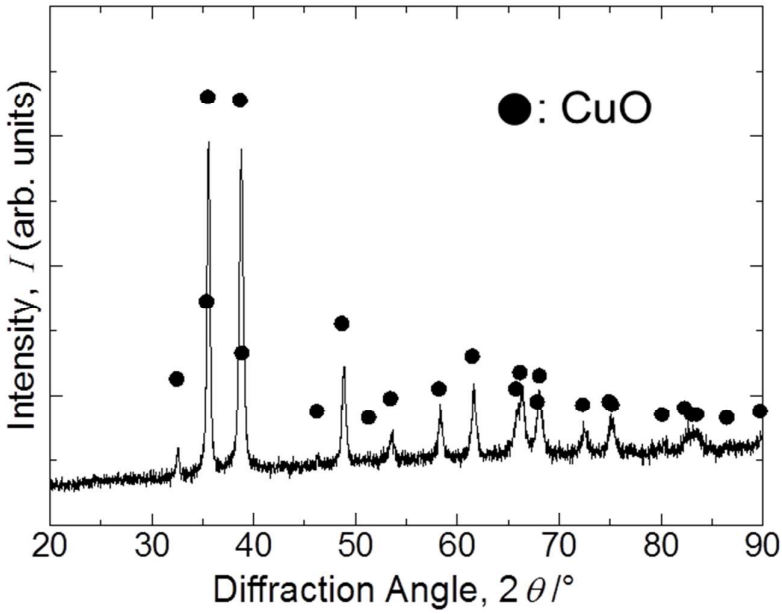

Figure S1. X-ray diffraction patterns of the sample calcined in argon at 800 °C followed by in air at 400 °C.

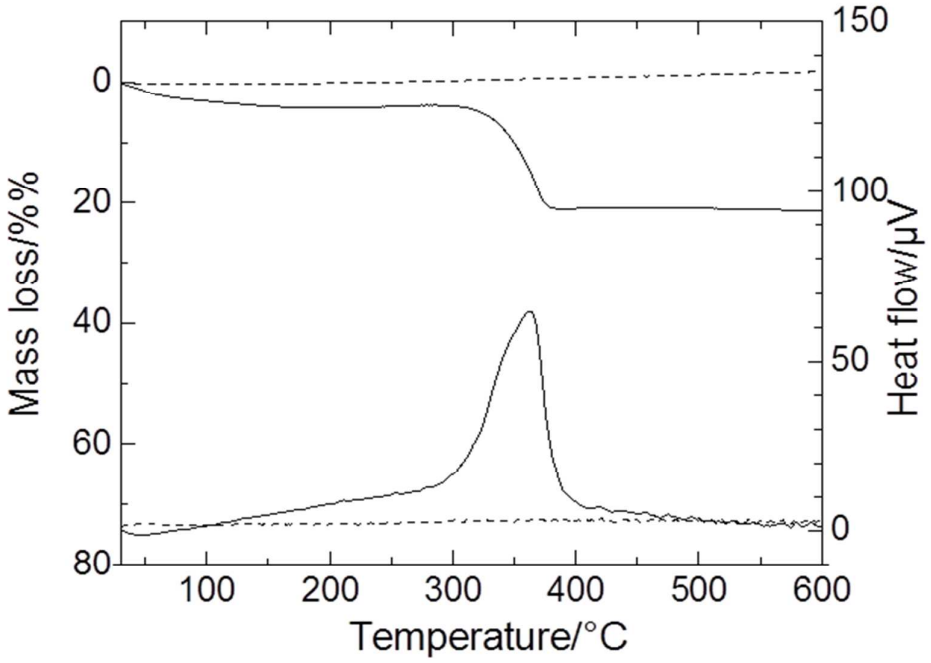

Figure S2. TG-DTA curves of the sample calcined in argon at 800 °C (solid line) and one calcined in argon at 800 °C followed by in air at 400 °C (dash line).

Direct preparation and conversion of copper-based monolithic xerogels with hierarchical pores

Table of contents

Glaphic:

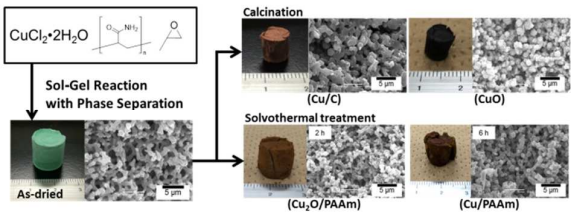

Text:

Copper hydroxide-based xerogels with hierarchical pores was prepared directly and changed to porous materials with different valence copper by heat-treatment.